Available online at www.sciencedirect.com
ScienceDirect
Archives of Biochemistry and Biophysics 453 (2006) 197–206
ABB
www.elsevier.com/locate/yabbi

A yeast sterol carrier protein with fatty-acid and fatty-acyl-CoA binding activity

Raúl G. Ferreyra [a,b,1], Noelia I. Burgardt [a,b,1], Daniel Milikowski [a,c], Gustavo Melen [d], Alberto R. Kornblihtt [b,d], Esteban C. Dell' Angelica [e], José A. Santomé [b,c], Mario R. Ermácora [a,b,*]

[a] *Departamento de Ciencia y Tecnología, Universidad Nacional de Quilmes, Bernal, Argentina*
[b] *Consejo Nacional de Investigaciones Científicas y Técnicas, Argentina*
[c] *Instituto de Química y Fisicoquímica Biológicas, Facultad de Farmacia y Bioquímica, Universidad de Buenos Aires, Ciudad de Buenos Aires, Argentina*
[d] *Departamento de Fisiología, Biología Molecular y Celular, Facultad de Ciencias Exactas y Naturales, Universidad de Buenos Aires, Ciudad de Buenos Aires, Argentina*
[e] *Department of Human Genetics, University of California at Los Angeles School of Medicine, Gonda Neuroscience and Genetics Research Center, Los Angeles, CA 90095-7088, USA*

Received 18 May 2006, and in revised form 29 June 2006
Available online 21 July 2006

Abstract

The 14-kDa sterol carrier protein 2 (SCP2) domain is present in Eukaria, Bacteria and Archaea, and has been implicated in the transport and metabolism of lipids. We report the cloning, expression, purification and physicochemical characterization of a SCP2 from the yeast *Yarrowia lipolytica* (YLSCP2). Analytical size-exclusion chromatography, circular dichroism and fluorescence spectra, indicate that recombinant YLSCP2 is a well-folded monomer. Thermal unfolding experiments show that SCP2 maximal stability is at pH 7.0–9.0. YLSCP2 binds *cis*-parinaric acid and palmitoyl-CoA with K_D values of 81 ± 40 nM and 73 ± 33 nM, respectively, sustaining for the first time the binding of fatty acids and their CoA esters to a nonanimal SCP2. The role of yeast SCP2 and other lipid binding proteins in transport, storage and peroxisomal oxidation of fatty acids is discussed.

Keywords: Yeast; Sterol carrier protein; *Yarrowia lipolytica*; Fatty-acid; Fatty-acyl-CoA; Lipid binding protein; Circular dichroism; Peroxisomes

Lipids pose a special challenge to cells because of their poor aqueous solubility and tendency to form micelles. It is believed that soluble lipid binding proteins (SLBP) alleviate the problem of intracellular storage and trafficking of lipids. Typical SLBP are fatty-acid binding protein (FABP), acyl-CoA binding protein (ACBP)[2], nonspecific lipid transfer protein (nsLTP), and sterol carrier protein 2 (SCP2). There are phylogenetic differences in the way cells handle lipids: FABP is found only in animals [1,2], ACBP in animals, yeasts, and plants [3], nsLTP only in plants [4], and SCP2 in all three domains of life [5]. This uneven distribution suggests some functional overlap between different SLBP.

Since long-chain fatty acids (LCFA) can readily cross membranes by passive diffusion and protein-mediated translocation [6], binding to ACBP, FABP and SCP2 targets these molecules into compartmentalized intracellular pools. Metabolic activation to the corresponding CoA

* Corresponding author. Fax: +54 114 365 7132.
E-mail address: ermacora@unq.edu.ar (M.R. Ermácora).
[1] These authors contributed equally to this work.
[2] *Abbreviations used:* ACBP, acyl-CoA binding protein; CD, circular dichroism; FABP, fatty-acid binding protein; IFABP, intestinal fatty-acid binding protein; LCFA, long-chain fatty-acid; LCFAcyl-CoA, long-chain fatty-acyl-CoA; nsLTP, nonspecific lipid transfer protein; PAGE, polyacrylamide gel electrophoresis; p-CoA, palmitoyl-CoA; PCR, polymerase chain reaction; PXP-18, peroxisomal polypeptide-18; SCP2, sterol-carrier protein-2; SDS, sodium dodecyl sulfate; SEC, size-exclusion chromatography; SLBP, soluble lipid binding protein; UV, ultraviolet; λ_{max}, wavelength of a spectral maximum.

0003-9861/$ - see front matter © 2006 Elsevier Inc. All rights reserved.
doi:10.1016/j.abb.2006.06.024

thioesters and binding of these to ACBP ensures retention. Thus, binding to SLBP and conversion into CoA esters establishes a concentration gradient of LCFA across the membrane and should influence transport for thermodynamic reasons [7]. Moreover, binding to a SLBP may prevent possible deleterious effects of free LCFA on membranes, signal transduction, and transcriptional control [6,8,9].

No member of the FABP family was ever found in yeasts [1,10–12], but these organisms have two SLBP: ACBP and SCP2 [13–15]. Notorious exception are *Saccharomyces cerevisiae* and *Schizosacharomices pombe*, which contains only ACBP [5]. Several years ago, we observed that whereas *Yarrowia lipolytica* grows well in a synthetic medium with sodium palmitate as the sole source of carbon and energy, *S. cerevisiae* does not. We hypothesized that the dissimilar behavior could be related to the presence of a LCFA binding activity in extracts of *Y. lipolytica* and its absence in *S. cerevisiae* [1,10]. Shortly after, we found that the activity of *Y. lipolytica* extracts was due to a 15-kDa basic protein, which could be purified in small amounts, digested and partially sequenced. At that time, based on the five short peptides sequenced, no significant similarity to other known protein was noticed [16]. At first we thought that the LCFA binding activity of *Y. lipolytica* was due to a new FABP, because ACBP does not bind LCFA [3] and PXP-18, a SCP2 protein isolated from *Candida tropicalis* cells grown exclusively on oleic acid [17] had been reported to lack that activity [18]. Later, however, using the partial sequence of this putative FABP for the design of degenerated primers, we retrieved from *Y. lipolytica* cells a cDNA encoding a polypeptide pertaining to the SCP2 family (YLSCP2; Milikowski et al., (2001) GenBank AJ431362). From this result it can be inferred that yeast SCP2 have LCFA binding capacity. A formal proof of this, however, is lacking, and the only activity reported so far for a yeast SCP2 is an in vitro chaperone-like protection of acyl-CoA oxidase [19].

There are striking differences between animal and yeast SCP2. In animals, SCP2 can be part of a variety of multidomain proteins—like the SCPX/proSCP2 and other multifunctional enzymes with dehydrogenase activity [20,21]. The SCPX/proSCP2 gene has two initiation sites and yields two separate mRNA: one encoding proSCP2, a 15-kDa precursor that is partly imported into peroxisomes and proteolytically cleaved to yield mature SCP2, and the other encoding SCPX, a peroxisomal branched-chain, 3-ketoacyl thiolase which carries proSCP2 at the C-terminus [22,23]. On the other hand, fungal SCP2 generally is a stand-alone, 14-kDa protein, seems to be strictly peroxisomal, and does not have a propeptide [5,18,24]. By analogy to animal SCP2, yeast SCP2 are believed to be involved the peroxisomal oxidation of LCFA.

Nowadays, several fungal SCP2 are known [5] and the complete genome of *Y. lipolytica* is available [25]. The function of SCP2 in yeast, however, was not further clarified. Moreover, the knowledge of the biochemical and physicochemical properties of yeast SCP2 is insufficient. Herein, we report the preparation of recombinant YLSCP2, its optical, hydrodynamic and thermodynamic characterization, and the study of its binding to *cis*-parinaric acid (PA) and palmitoyl-CoA (p-CoA).

Materials and methods

General details

Amino acid sequencing was performed with an Applied Biosystems 477A (Foster City, CA) protein sequencer and a 120A phenylthiohydantoin analyzer. Electrospray mass analysis was conducted on a VG Biotech/Fisons (Altrincham, UK) triple-quadrupole spectrometer. Analytical size-exclusion chromatography (SEC) was carried out by FPLC on a Superose 12 column (Pharmacia, Uppsala, Sweden). Elution buffer was 50 mM sodium phosphate, pH 7.0 (Buffer A), and UV detection was at 280 nm. Stokes' radii (R_S) were calculated as described [26]. Origin (Microcal Software Inc., Northampton MA, USA) was used to fit equations to experimental data. All chemicals were of the purest analytical grade available. Alignment of protein sequences was performed with ClustalX [27], using default parameters. Molecular visualization and calculations were performed with MOLMOL 2k.2 (http://www.mol.biol.ethz.ch/groups/wuthrich_group). Recombinant intestinal fatty-acid binding protein (IFABP) was expressed and purified as previously described [28]. Antibodies against YLSCP2 were generated in white rabbits by injections of pure recombinant YLSCP2 (0.2 mg emulsified in complete Freund's adjuvant). Secondary structure content was estimated using DICROPROT [29].

Yeast strains and culture media

Yeast strains were *S. cerevisiae* MMY2 MAT α-*ura3* and *Y. lipolytica* CX-121-1B *ade2*, from the personal collection of Professor J.R. Mattoon (University of Colorado Springs, CO, USA). Culture media were: (a) modified VJ minimal medium [1]; (b) YPD (1% peptone, 1% yeast extract and 0.2% glucose); (c) LB (tryptone 10 g/L, yeast extract 5 g/L, NaCl 10 g/L). Yeast was grown aerobically at 30 °C in (a) modified VJ minimal medium containing either 0.1% sodium palmitate or 0.1% glucose, (b) LB, or (c) LB containing 0.1% sodium palmitate.

Molecular biology

The YLSCP2 gene was amplified directly from genomic DNA using the primers 'GTTTAGCTCCCCAGAATA TC' and 'GTTGCGGATCCAATATAGTAAATCATC'. *Nde*I and *Bam*HI restriction sites incorporated by an additional primer allowed oriented ligation into the polylinker of pET9b (Invitrogen, San Diego, CA, USA) yielding pYLSCP2. For preparative purposes, the expression vector was amplified in *Escherichia coli* JM109 cells. Colonies were

selected on LB-agar plates containing 50 μg/ml of kanamycin, and positive clones identified by PCR with gene- and vector-specific primers. The plasmid was sequenced to establish the identity of the insert.

Protein expression and purification

Escherichia coli BL21 (DE3) cells were transformed with pYLSCP2 and grown to saturation (overnight; 37 C; LB broth containing 50 mg ml^{-1} kanamycin). The culture (10 ml) was used to inoculate 1000 ml of LB, and the growth was continued to $A_{600\text{nm}} \sim 1.0$. Then, either 1 mM IPTG or 1% lactose was added to induce protein expression. After 3-h induction, cells were harvested by centrifugation at 5000*g* (10 min; 4 °C), and the resulting pellet was stored at −20 °C. For protein purification, harvested cells (~5 g) were suspended in 10 ml of lysis buffer (50 mM Tris–HCl, 100 mM NaCl, 1.0 mM EDTA, and pH 8.0) and disrupted by pressure (1000 psi; French Pressure Cell Press; Thermo IEC, Needham Heights, MA, USA). Inclusion bodies were isolated by centrifugation (15,000*g*, 10 min at 4 °C). Several contaminants were removed from the inclusion bodies by suspension in 5 ml of lysis buffer, conditioning and centrifugation. Conditioning treatments were: (a,b) 0.2 mg ml^{-1} lysozyme, 10 mM $MgCl_2$, 10 μg ml^{-1} DNase I, 30 min at 37 °C; (c) 0.5% Triton X-100, 10 min at room temperature; and (d–f) distilled water. The conditioned pellets were stored at −20 °C until further purification. Inclusion bodies were solubilized by incubation in 25 mM sodium acetate, pH 5.5, 8 M urea, 10 mM glycine (Buffer B) for 1 h in an orbital shaker. The solution was clarified by centrifugation at 15,000*g* for 15 min at 4 °C, and loaded into a SP Sepharose Fast-Flow (Pharmacia Biotech, Uppsala, Sweden) cationic exchange column (1.5 × 3.0 cm) equilibrated with Buffer B. Protein elution was performed with a 200-ml linear gradient between 0 and 500 mM NaCl in Buffer B and monitored by absorbance at 280 nm and SDS–PAGE. Fractions containing pure YLSCP2 were pooled and stored in aliquots at −20 °C. Refolding was carried out by dialysis (16 h) at 5 °C against 1000 volumes of Buffer A. Finally, particulate matter was removed by centrifugation (16,000*g*, 20 min at 4 °C).

To obtain a partially purified YLSCP2 from *Y. lipolytica*, cells were suspended in 20 mM sodium phosphate, 1 mM EDTA, pH 7.0 (Buffer C), and disrupted with a French press as described above except that the pressure was set to 2000 psi. Particulate material was removed by centrifugation at 15,000*g*, 20 min at 4 °C, and the supernatant was subjected to preparative size-exclusion chromatography on a Sephacryl S100 HR column (Pharmacia Biotech, Uppsala, Sweden; 2.5 × 90 cm column) equilibrated in Buffer C. Chromatographic fractions were monitored by UV absorption and western blotting. The fractions that contained YLSCP2 were further purified by ionic exchange chromatography as above with a gradient of 0–500 mM NaCl in Buffer C. Finally, for mass analysis and N-terminal sequencing, the protein was further purified on a reverse-phase HPLC column (Delta-Pak C_4; 5 μm, 300 Å, 3.9 × 150 mm; Waters Corporation, Milford, MA, USA) using a gradient of 0.5% min^{-1} between 0.05% trifluoroacetic acid (v/v) and 75% acetonitrile, 0.05% trifluoroacetic acid (v/v/v).

Equilibrium unfolding

Thermal transitions as a function of temperature were monitored by circular dichroism (CD) at 220 nm. Protein concentration was 3.1 μM in 50 mM phosphoric acid adjusted to pH 5.0, 7.0 and 9.0 with sodium hydroxide. A 1.0-cm cell was used. Temperature was varied 2 °C min^{-1}, from 0 to 80 °C, and the melting curve was sampled at 0.5 °C intervals. Assuming a two-state equilibrium, $N \leftrightarrow U$, data were fitted to the following equations [30]:

$$\Delta G_{NU} - RT \ln\left(\frac{f_U}{f_N}\right) = \Delta H_{T_m} + \Delta C_P(T - T_m) - T\left(\left(\frac{\Delta H_{T_m}}{T_m}\right) + \Delta C_P \ln\left(\frac{T}{T_m}\right)\right) \quad (1)$$

$$S = f_N(S_{0,N} + l_N T) + f_U(S_{0,U} + l_U T) \quad (2)$$

where f_U and f_N are the unfolded and folded fractions, T_m is the temperature at which $f_U = f_N$, S is the observed CD signal, $S_{0,N}$ and $S_{0,U}$ are the intrinsic spectroscopic signals for the native and unfolded state, respectively, and l_N and l_U are the slopes for the assumed linear dependence of $S_{0,N}$ and $S_{0,U}$ with the temperature, respectively.

Optical studies

Unless otherwise indicated, samples for spectroscopy were in Buffer A. Ultraviolet (UV) absorption was measured with a Shimadzu UV-160A spectrophotometer (Shimadzu Corporation, Japan). Extinction coefficient determination was as previously described [31]. Circular dichroism (CD) measurements were carried out at 20 °C, on a Jasco 810 spectropolarimeter (Jasco Corporation, Japan) equipped with a Peltier-effect device and calibrated with (+)-10-camphorsulfonic acid. Scan speed was set to 20 and 50 nm/min (near-UV and far-UV, respectively) with a response time of 1 s, 0.2 nm pitch and 1 nm band width. Near-UV measurements were done with 1.0 cm cells containing 53 μM protein. In the far-UV, 0.1 cm cells were used and protein concentration was 13 μM. Six spectra were acquired and averaged for each sample. Fluorescence measurements were done with an ISS K2 flourometer (ISS, Champaign, IL, USA). Slits of 8-nm were used for excitation and emission.

Binding of cis-parinaric acid and p-CoA

The experiments were carried out in Buffer A with a 10.0-mm path quartz cuvette thermostatted at 20 °C.

Ligand addition was incremental, and each measurement was preceded by 2-min incubation in the cell holder. A quantum counter in the reference channel was used to correct for lamp fluctuations. *cis*-Parinaric acid and p-CoA were from Molecular Probes (Eugene, OR, USA) and Sigma Chemical Co (Saint Louis, MO, USA). For *cis*-parinaric acid binding, a fresh stock solution of the lipid in ethanol ($\varepsilon_{304\text{nm}} = 78{,}000\ \text{M}^{-1}\,\text{cm}^{-1}$ [32]) was diluted in Buffer A and used for the titration of 1 μM protein solutions; the extent of binding was assessed by the change in fluorescence emission at 430 nm upon excitation at 325 nm. For p-CoA binding, a stock solution of the thioester ($\varepsilon_{260\text{nm}} = 14{,}700\ \text{M}^{-1}\,\text{cm}^{-1}$ [33]) was prepared in Buffer A, protein solution was 5 μM, and emission at 326 nm upon excitation at to 294 nm was monitored.

Binding constants were calculated using a quadratic equation for single-site binding [34],

$$PL = \frac{(P_0 + L_0 + K_D) - \sqrt{(P_0 + L_0 + K_D)^2 - 4P_0L_0}}{2}, \qquad (3)$$

where PL, P_0, L_0 and K_D are the concentrations of complex, total protein, total ligand and dissociation constant, respectively.

For *cis*-parinaric acid binding, measured signal is related to the concentration of complex and free ligand by

$$y = Y_L(L_0 - PL) + Y_{PL}PL, \qquad (4)$$

where Y_L and Y_{PL} are the signals for the free ligand and the complex, respectively. For p-CoA, the measured signal is

$$y = Y_P(P_0 - PL) + Y_{PL}PL, \qquad (5)$$

where Y_P and Y_{PL} are the signals for the free protein and the complex, respectively.

Results and discussion

Cloning and sequence analysis

Using PCR and starting from total DNA, the *Y. lipolytica* SCP2 gene was cloned. The sequence is in full agreement with that reported for the SCP2 gene of the strain CLIB122 YALI0E01298g; [25]), which eliminates the conflict regarding four base pairs of our previously deposited sequence (GenBank AJ431362).

The ancestral SCP2 evolved through a series of fusion and fission events, which led to a large variety of multidomain and unfused proteins in different subcellular compartments [5]. A bioinformatic search yielded more than 200 SCP2 protein domains, belonging to species from Eukaria, Bacteria and Archaea. For comparison, we aligned 34 representative sequences (not shown). YLSCP2, like most fungal SCP2, is a single-domain protein [5]. Its sequence is most similar to those of *Neurospora crassa*, *Aspergillus fumigatus*, *Botryotinia fuckeliana*, and *Aspergillus nidulans* SCP2 (53–57% amino acid identity). YLSCP2 is also closely related to SCP2 from other fungi and to multicellular eukaryotic SCP2 (38–52% and 20–28% amino acid identity, respectively). Very interestingly, the SCP2 from Archaea and Bacteria have 17–29% of their residues identical to those of YLSCP2. The sequence similarity among SCP2 domains is evident, especially at the C-terminus, suggesting that the evolution of this protein is constrained by stringent functional and/or structural requirements.

SCP2 X-ray structures from bacteria, insects, and mammals are available (see Ref. [20,35,36] and PDB 2CX7). A condensed alignment, showing YLSCP2, SCP2 with known three-dimensional structure, and examples from the three domains of life is shown in Fig. 1. Superposition

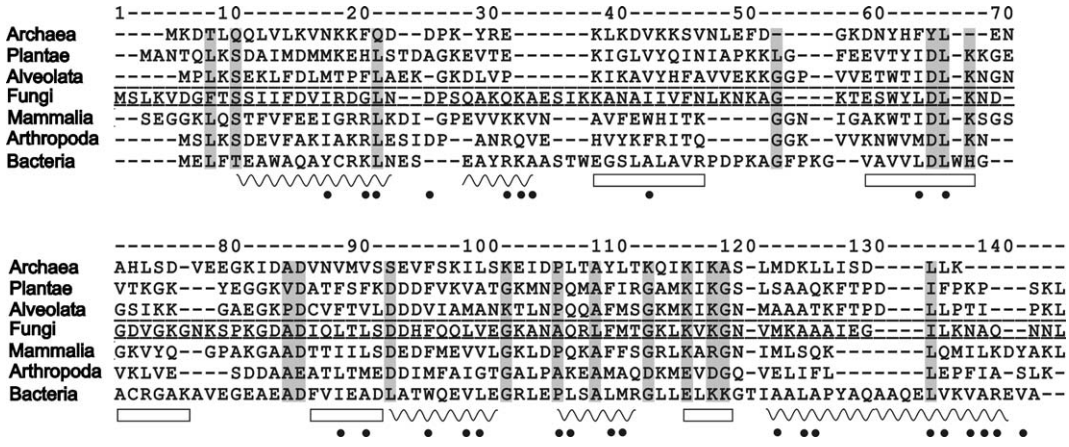

Fig. 1. Alignment of seven representative SCP2 sequences from the three domains of life. Archaea (Q97CR7; *Thermoplasma volcanium*), Bacteria (Q72LM5; *Thermus thermophilus*, strain HB27), Plantae (Q9FMN0; *Arabidopsis thaliana*), Fungi (P80547; *Yarrowia lipolytica*; YLSCP2), Mammalia (P51659; *Homo sapiens*; Peroxisomal multifunctional enzyme type 2) and Arthropoda (Q86PR3; *Aedes aegypti*) are shown. The alignment was refined manually to take into account the structural correspondence observed in the crystal structures of bacterial (2CXT), arthropodal (1PZ4), and mammalian (1IKT) SCP2 domains. Horizontal lines highlight the YLSCP2 sequence. α-helical and β segments in all three crystal structures are indicated by wavy lines and boxes, respectively. Dots identify the residues of the arthropodal and mammalian proteins involved in binding of C16 fatty-acid and Triton X-100, respectively ([20,36]; Fig. 2). Shaded positions correspond to highly conserved residues (5–7 identical residues). Accession numbers and entry names are from Uniprot (PIR) or PDB.

of the X-ray structures indicates a strong fold similarity (Fig. 2). Indeed, after superposition of the structurally equivalent residues the RMSD between human and insect SCP2 (1IKT and 1PZ4, respectively) is only 1.15 Å. Likewise, de RMSD between insect and bacterial SCP2 (2CX7) is 3.4 Å.

The structural information was taken into account for the manual refinement of the sequence alignment shown in Fig. 1. The alignment provides a unified view of the entire SCP2 family and constitutes a good starting point for modeling sequence–structure–function relationships. For instance, the structural comparison and sequence alignment reveal a common set of residue positions most likely to be involved in the binding to hydrophobic ligands (Figs. 1 and 2). These residues line the tunnel-shaped binding cavity observed in the X-ray structures and in most cases have preserved side chain properties at each position.

The comparison revealed an interesting detail: in bacterial SCP2 the C-terminal helix is longer than in mammalian and arthropodal SCP2 and partially obstructs the binding cavity (Figs. 1 and 2). In the NMR structure of *Thermus thermophilus* HB8 SCP2 (PDB 1WFR) the last portion of the C-terminal helix is frayed. Likewise, in the NMR model of rabbit SCP2 the C-terminal helix is poorly defined [37,38]. Taken together, these observations offer support for the proposal that the C-terminal helix modulates the access to the binding cavity [35].

According to a neural network based method [39], YLSCP2, as well as most fungal SCP2, are predicted to be *N*-acetylated; and, as shown below, this showed to be the case for YLSCP2. Also, as in most SCP2 domains, the three C-terminal YLSCP2 residues, 'NNL', are compatible with the 'peroxisome targeting signal 1' (PST-1), which is part of the determinants that direct proteins to that organelle [40].

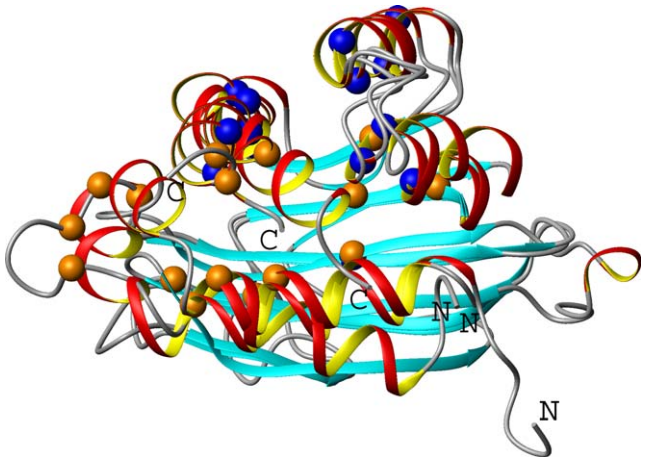

Fig. 2. X-ray SCP2 structures. Bacterial (2CXT), arthropodal (1PZ4), and mammalian (1IKT) SCP2 domains were superposed minimizing the RSMD of common secondary structure elements. The N- and C-termini are indicated. The α carbon of residues involved in binding to lipids [20,36] are shown as blue (1IKT) and orange (1PZ4) spheres.

Protein expression and purification

The cDNA encoding YLSCP2 was cloned into pET-9b originating pYLSCP2. Upon induction with IPTG, *E. coli* BL21 (DE3) cells harboring pYLSCP2 express YLSCP2 as inclusion bodies with high yields (20 mg/L of culture). After a single ionic-exchange chromatography of inclusion bodies solubilized by concentrated urea, YLSCP2 is obtained >95% pure, and its refolding is accomplished by dialysis. Spectrometry showed that recombinant SCP2 has the mass expected from sequence within 1.5 Da. In addition, N-terminal Edman degradation confirmed that the initial methionine is removed posttranslationally.

Polyclonal antibodies raised in rabbits immunized with purified recombinant YLSCP2 reacted in a Western blot with a ~14 kDa protein from extracts of *Y. lipolytica* grown on sodium palmitate (Fig. 3). Cells grown on glucose tested negative in the assay, which confirmed the inducible nature of the protein [16]. The same behavior was reported for PXP-18, the SCP2 protein from *C. tropicalis* [18].

Western blotting allowed monitoring the expression of the protein induced in *Y. lipolytica* under different conditions (not shown). Although cells growing on VJ minimal medium express the protein, it was found that a richer medium like LB increases significantly its production. In both cases, however, induction with sodium palmitate remained essential [16]. Due to the increased expression in LB, and using the protocol developed for *E. coli* extracts, the induced protein could be easily purified from yeast

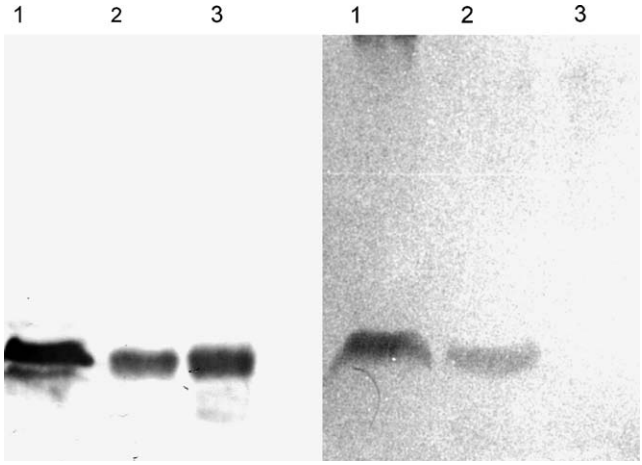

Fig. 3. Expression of YLSCP2 in *Yarrowia lipolytica* cells monitored by Western blotting. The polyclonal antibody utilized was from rabbits immunized with recombinant YLSCP2. Left panel: Lane 1, whole yeast extract of cells grown on VJ minimal medium with 0.1% sodium palmitate. Lanes 2 and 3, 50 and 100 ng of purified recombinant YLSCP2, respectively. Right panel: Lane 1, whole yeast extract of cells grown on modified VJ minimal medium supplemented with 0.1% sodium palmitate. Lane 2, ionic exchange fraction of the yeast extract analyzed in the previous lane. Lane 3, whole extract of cells grown on modified VJ minimal medium supplemented with 0.1% glucose. Molecular markers (not shown) indicate that the bands revealed in both panels correspond to a protein of ~14 kDa.

extracts. Mass spectrometry confirmed within 0.5 mass units that the induced protein is YLSCP2. The result indicated that the induced YLSCP2 has the initial methionine removed and the following serine *N*-acetylated. Unlike the recombinant YLSCP2 expressed in *E. coli*, the protein produced by the yeast was impervious to Edman degradation, in accordance with the proposed N-terminal blocking. This finding confirmed our previous report [16].

Hydrodynamic study

The aggregation state of purified recombinant YLSCP2 was assessed by analytical size-exclusion chromatography [41]. The elution profile at 20 °C in 100 mM sodium phosphate, pH 7.0 (Fig. 4) was consistent with a monodisperse population of molecules having a Stokes' radius of 21.1 Å. Since the theoretical value for a monomeric spherical protein the size of YLSCP2 is 18.8 Å and a dimer has a minimal theoretical radius of 24.2 Å, it is concluded that YLSCP2 is monomeric in solution.

Optical studies

The extinction coefficient of YLSCP2 was found to be $6{,}986 \pm 41\ M^{-1}\ cm^{-1}$ ($n = 3$), which is close to the theoretical value for the unfolded protein [42]. CD spectra of native YLSCP2 are shown in Fig. 5. α-Helical features dominate the far-UV spectrum: two minima centered at 220 and 208 nm ($n\pi^*$ and $\pi\pi^*$ transitions, respectively),

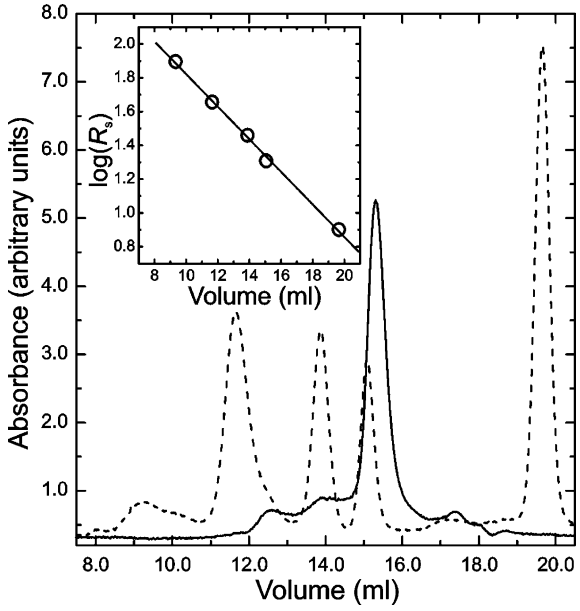

Fig. 4. Analytical SEC. The elution profile of native YLSCP2 is shown as a solid line. Thyroglobulin (670 kDa), bovine globulin (150 kDa), chicken ovoalbumin (44 kDa), equine myoglobin (17 kDa) and vitamin B12 (1.35 kDa) were used to calibrate the column (dashed line). The empirical relationship between molecular weight and R_s [26] and the elution volume of each standard was used to construct the calibration curve shown in the inset. The elution volume and peak shape of YLSCP2 are consistent with a monomeric native state (see the text).

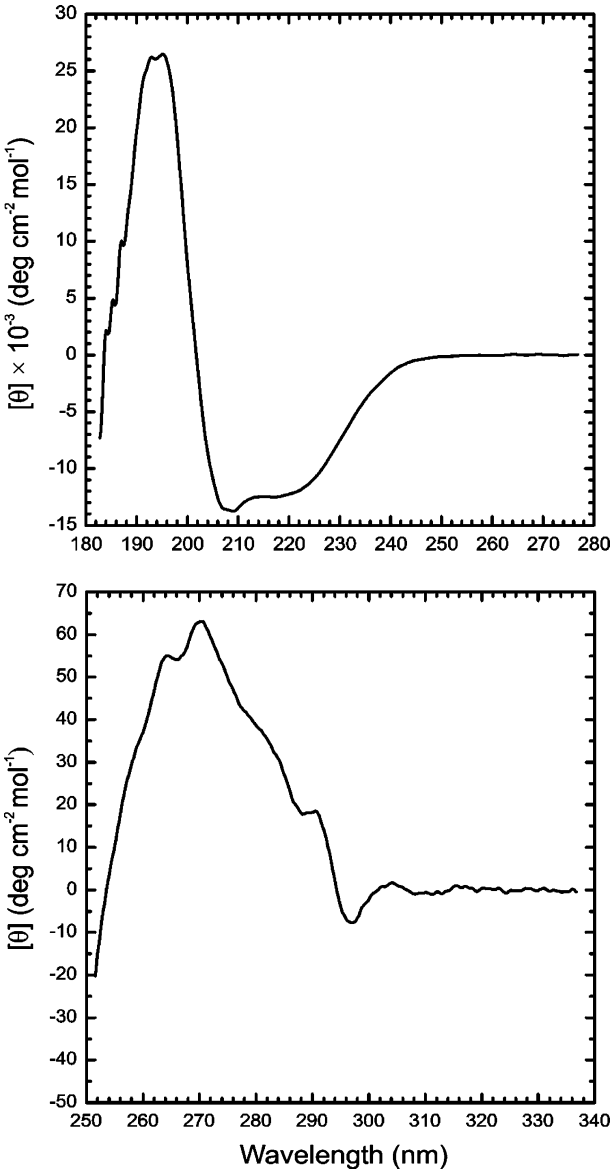

Fig. 5. Far- and near-UV-CD spectra of YLSCP2. Measurements were performed at 20 °C in Buffer A.

and one maximum centered at 194 nm ($\pi\pi^*$ transition). In accordance with the structural similarity among all SCP2 proteins inferred from the sequence analysis, the far-UV-CD spectrum of YLSCP2 is very similar to that of recombinant human SCP2 [43]. YLSCP2 content of secondary structure was computed using a suite of four programs included in DICROPROT [29] yielding 28–39% and 11–22% for α and β structure, respectively. These figures are in reasonable agreement with the observed content of each secondary structure in the crystallographic models of SCP2 (36–41% and 25–28% for α and β structure, respectively).

The intense and highly structured near-UV-CD spectrum of YLSCP2 suggests a well-ordered tertiary structure and a rigid asymmetric environment for the aromatic residues. The vibronic structure of phenylalanine residues can

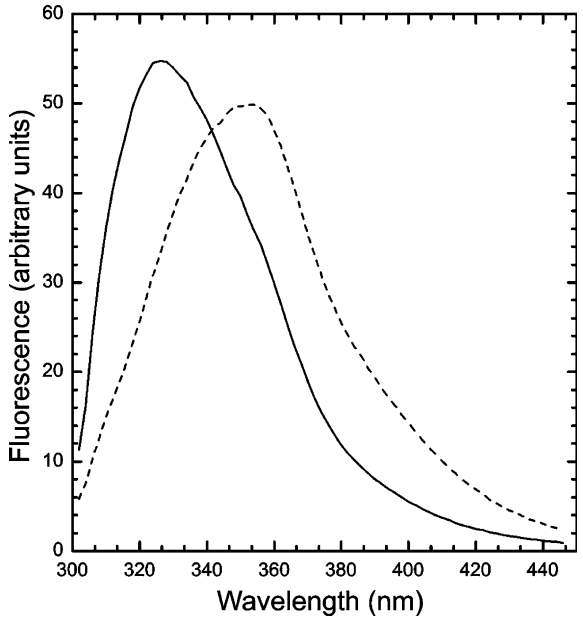

Fig. 6. Fluorescence emission spectra of YLSCP2. Solid line, native state (Buffer A). Dashed line, unfolded state (Buffer A plus 7.0 M urea). Protein concentration and excitation wavelength were 10.5 μM and 294 nm, respectively.

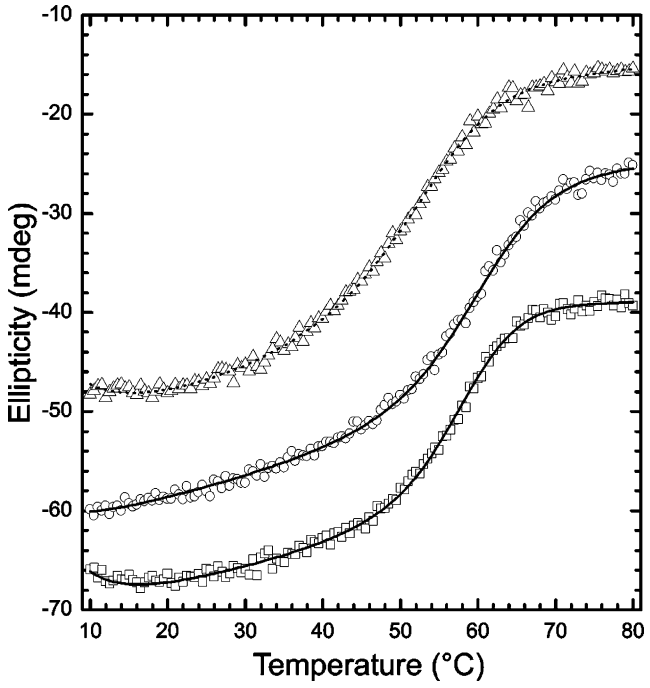

Fig. 7. Thermal unfolding of YLSCP2. CD signal at 220 nm was monitored as the temperature was linearly increased 2 °C min^{-1}. For clarity, curves have been arbitrarily displaced on the vertical axe. Triangles, circles, and squares are data from runs performed at pH values of 5.0, 7.0 and 9.0, respectively. Thermodynamic parameters derived from the each fit (lines) are shown in Table 1.

be noticed at 264 and 270 nm. Likewise, Tyr 56 and Trp 55, originate bands at ~285, 290 and 295 nm. To our knowledge, this is the first report of the near-UV spectrum for an SCP2 protein. Since tryptophan and tyrosine residues are rare in SCP2 proteins (not shown) and mostly at conserved positions, near-UV-CD analysis may turn into a very useful tool to study the SCP2 family structure and function.

Fluorescence spectra of native and urea unfolded YLSCP2 are shown in Fig. 6. In the native state, upon excitation at 294 nm, the peak of emission is centered at 326 nm, which indicates that Trp 55 is shielded from the solvent and in an overall nonpolar environment. Urea-induced unfolding brings about a moderate decrease in fluorescence intensity and a shift in the emission peak to 354 nm. The spectrum of unfolded YLSCP2 is superimposable to that of free tryptophan (not shown).

Equilibrium unfolding

The thermal unfolding of YLSCP2 at three different pH values was assessed measuring optical ellipticity as a function of temperature (Fig. 7). Unfolding was >70% reversible judging from the recovery of the signal upon cooling (not shown). The results are summarized in Table 1. At pH 7.0, T_m is 60 °C and $\Delta G^{25°C} = 2.2$ kcal mol^{-1}, which indicates that YLSCP2 is well-folded at room temperature. A decrease of 8 °C in T_m and a significant loss of stability occur at pH 5.0. At pH 9.0 both T_m and $\Delta G^{25°C}$ are similar than at pH 7.0. The stability of YLSCP2 in alkaline solutions is of physiological interest because the pH of the peroxisomal lumen of yeasts growing on LCFA was reported

Table 1
Thermal unfolding parameters of YLSCP2[a]

pH	T_m	ΔC_P	ΔH_{T_m}	$\Delta G^{25°C}$
5.0	51.30 ± 0.20	1.23 ± 0.02	32.97 ± 0.58	1.32 ± 0.02
7.0	59.25 ± 0.21	1.20 ± 0.02	42.33 ± 0.58	2.17 ± 0.02
9.0	57.36 ± 0.12	1.76 ± 0.01	51.17 ± 0.37	2.11 ± 0.03

[a] The data shown in Fig. 5 were analyzed using Eqs. (1) and (2). Units are: T_m, °C; C_p, kcal mol^{-1} K^{-1}; H,G, and S, kcal mol^{-1}. T_m is the melting temperature at which the transition occurs with $\Delta G = 0$. Errors are standard deviations calculated splitting the data randomly in three sets and performing separate fits.

to be >8.0 [44]. Nevertheless, the thermal unfolding of YLSCP2 might be incomplete for the observed ΔC_P of 1.20 ± 0.02 kcal mol^{-1} K^{-1} is also lower than expected for a protein of this size [45], as if unfolding would have exposed only a fraction of the internal surface. Since virtually no data on the dynamic and equilibrium of folding of proteins having the YLSCP2 topology are available, the partially folded state of YLSCP2 is being further characterized in our laboratory as an important model for protein folding in general.

Lipid binding

As reported for other SLBP [32], binding of *cis*-parinaric acid to YLSCP2 results in a large increase of fluorescence emission at 410 nm (Fig. 8). Isothermal titration of YLS-

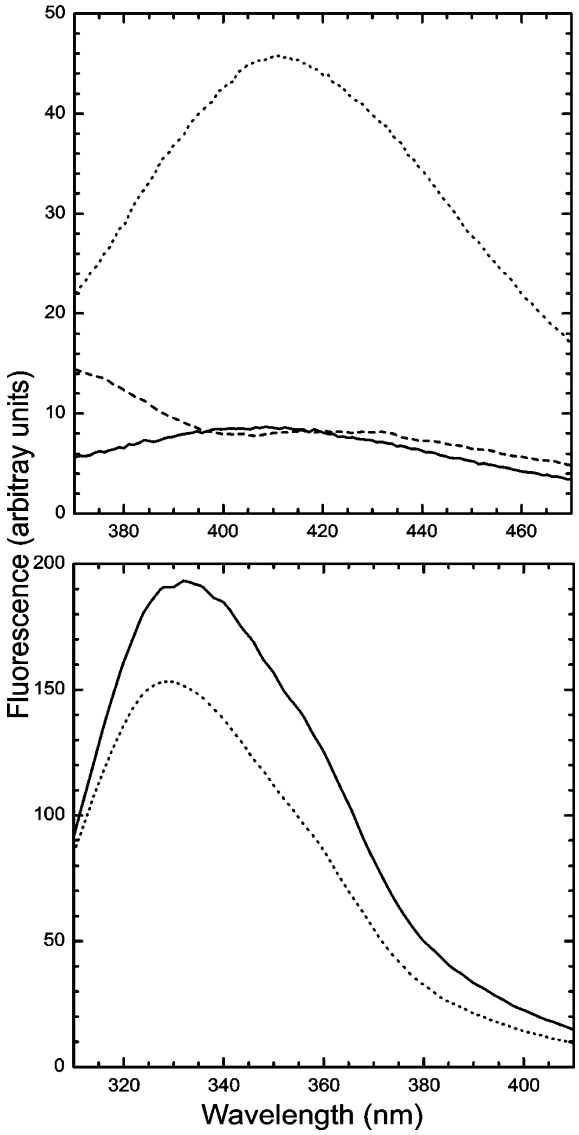

Fig. 8. Effects of binding on fluorescence. Upper panel: 2.6 μM *cis*-parinaric acid (solid); 0.9 μM YLSCP2 (dashes); 0.9 μM YLSCP2 plus 2.6 μM *cis*-parinaric acid (dots); excitation was at 307 nm. Lower panel: 10 μM YLSCP2 (solid line); 10 μM YLSCP2 plus 23 μM p-CoA (dots); excitation was at 290 nm.

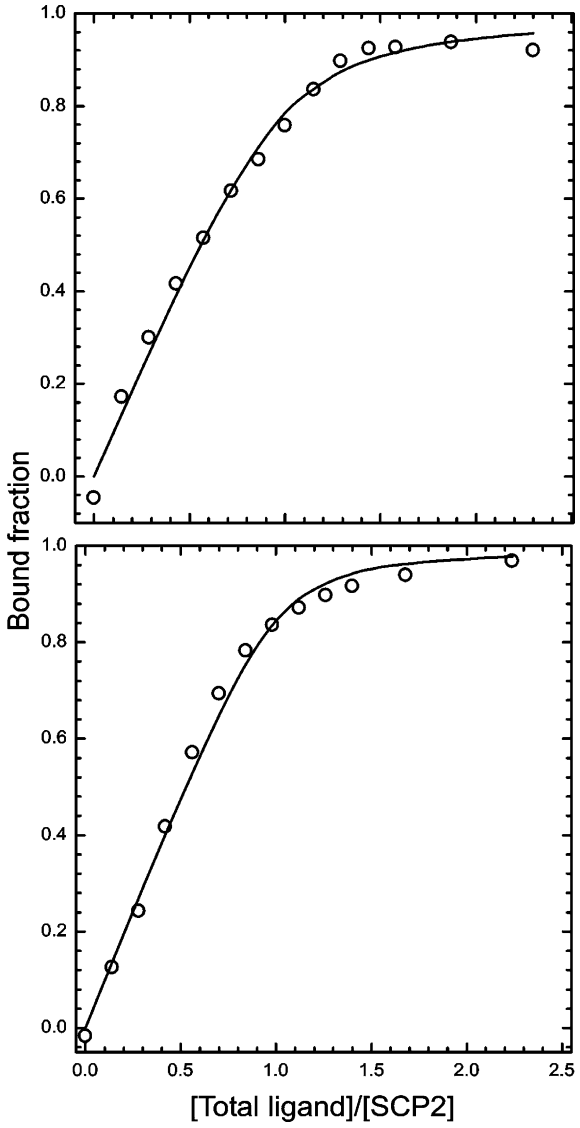

Fig. 9. Titration of YLSCP2 with *cis*-parinaric acid (upper panel) or p-CoA (lower panel). Protein concentration was 0.1–1 μM, and binding was monitored by fluorescence (see Fig. 8). The concentration of the species at equilibrium was calculated according to Eqs. (3)–(5). K_D values are reported in the text.

CP2 with *cis*-parinaric acid monitored by fluorescence (Fig. 9) allowed to calculate a K_D of 81 ± 40 nM (mean ± SE; $n = 2$), a value comparable to that reported recombinant human SCP2 (160–180 nM; [46–49]). As a control, the same procedure was applied to intestinal FABP (not shown), resulting in a K_D of 52 ± 70 nM (mean ± SE; $n = 2$). The value obtained for IFABP is also in general agreement with previous reports [50].

Binding of p-CoA to YLSCP2 brings about a decrease in fluorescence (Fig. 8), which implies that Trp 55 is either close to the binding pocket or sensing a conformational change related to binding. This decrease in fluorescence was profited to measure directly the affinity for p-CoA (Fig. 9), yielding a K_D of 73 ± 33 nM (mean ± SE; $n = 3$). Previously reported values for the K_D of binding of *cis*- and *trans*-parinoyl-CoA to recombinant human SCP2 are 4.6 and 2.8 nM, respectively [46]. It is clear that the affinity of YLSCP2 and human SCP2 for LCFAcyl-CoA is very high; however whether the difference in their K_D values is significant remains to be seen because the differences in methodology and lipid chain preclude direct comparison.

Biochemical considerations

Although free diffusion can account for a substantial fraction of LCFA uptake in higher eukaryotic cells, almost all aspects of LCFA traffic are stimulated 2- to 200-fold by SLBP; moreover, these proteins modulate expression of specific genes related to lipid metabolism [51]. Animal

tissues contain several FABP—in some cases within the same cell type—which, along with SCP2, expand considerably the intracellular pool of diffusible LCFA. In specialized cells, FABP constitute up to 5% of the soluble protein, and their functional role has been highlighted by several genetic knock-out experiments. These experiments also demonstrated that the lack of a given FABP is frequently compensated by overexpression of another protein with LCFA binding capacity [9].

The results reported herein show that YLSCP2 affinity for LCFA is comparable to that of a typical FABP. No member of the FABP family is known in yeasts, and although some of these microorganisms contain ACBP, this protein does not bind unesterified LCFA [3]. SCP2 may be an alternative carrier for unesterified LCFA. However, it was reported that (a) *S. cerevisiae* exhibits normal metabolism of lipids despite naturally lacking both SCP2 and FABP [52] and (b) *C. tropicalis* SCP2 is targeted almost exclusively to the matrix of peroxisomes [24]. Thus, in these yeasts the cytoplasmic pool of diffusible LCFA seems to be limited to submicellar concentrations. This is in striking contrast with the animal cytoplasm where the concentration of LCFA can expand following the expression of FABP.

The above considerations suggest that a soluble protein carrier may be advantageous but nonessential for cytoplasmic LCFA trafficking. Nonetheless, if the absence of SCP2 in the cytoplasm of *Y. lipolytica* is confirmed, it would be interesting to study how this yeast achieves its astonishing capacity of consuming large amounts of LCFAs [53]. It must be emphasized that the possession of a soluble LCFA activity circumscribed to a single organelle and to a single protein would make *Y. lipolytica* an extremely promising system to study lipid metabolism, especially using genetic approaches and in comparison with *S. cerevisiae*.

Metabolic trapping into acyl-CoA esters is the first step in the formation of the concentration gradient that extracts LCFA from membranes. This process, defined as 'vectorial acylation' and by which import and activation are linked to each other, includes binding to pool-former proteins that feed the substrate to the metabolic sink [52]. In animals, cytoplasmic acyl-CoA binding activity is due to ACBP and SCP2, whereas SCP2 plays that role in peroxisomes. We report herein that YLSCP2 affinity for p-CoA is similar to that of the animal counterpart, and, therefore, YLSCP2 may function as the peroxisomal acyl-CoA pool-former in yeast.

It is believed that peroxisomal SCP2 participates in LCFA oxidation by facilitating the interaction of the corresponding enzymes with their substrates. Interestingly, a direct interaction of SCP2 with acyl-CoA oxidase has been demonstrated [54]. To our best knowledge, SCP2 knock-out in yeast has not been performed, and the function of yeast SCP2 in LCFA metabolism can be inferred only from the observation of wild-type phenotypes and from the biophysical properties of the molecule. In *S. cerevisiae*, which naturally lacks SCP2, LCFA are predominantly transported in their activated form into the peroxisomal lumen by the Pxa1p–Pxa2p heterodimer [52]. Moreover, whereas animal cells constitutively express SCP2, yeasts do so only upon induction by LCFA. These facts, along with the exclusively peroxisomal nature of yeast β-oxidation [52], suggest that SCP2 is a crucial player in high-throughput peroxisomal LCFA oxidation in yeasts.

Concluding remarks

Although the ubiquity and structural conservation of SCP2 domains seems hardly accidental, the knowledge of their general role in lipid traffic and metabolism is still lacking. This work provides evidence of the ability of nonanimal SCP2 to bind fatty acids and their CoA esters, which suggests at least one common function in all living organisms. The preparation of pure recombinant YLSCP2 and characterization of its basic structural and biochemical properties reported herein will help to design detailed comparative studies aimed to unveil how lipid binding to SCP2 influences the metabolism of different cells and the molecular basis of SCP2 function.

Acknowledgments

This work was supported by Grants from Agencia Nacional de Promoción Científica y Técnica, Universidad Nacional de Quilmes, Third World Academy of Sciences, and Fundación Antorchas. We thank Professor J.R. Mattoon for providing the *Y. lypoytica* strain utilized in this work.

References

[1] E.C. Dell'Angelica, C.A. Stella, M.R. Ermácora, E.H. Ramos, J.A. Santomé, Comp. Biochem. Physiol. B 102 (1992) 261–265.
[2] J.A. Santomé, S.M. Di Pietro, B.M. Cavagnari, O.L. Córdoba, E.C. Dell' Angelica, Trends Comparative Biochem. Physiol. 4 (1999) 23–38.
[3] B.B. Kragelund, J. Knudsen, F.M. Poulsen, Biochim. Biophys. Acta 1441 (1999) 150–161.
[4] J.-C. Kader, Annu. Rev. Plant. Physiol. Plant. Mol. Biol. 47 (1996) 627–654.
[5] J. Edqvist, K. Blomqvist, J. Mol. Evol. 62 (2006) 292–306.
[6] A.W. Zimmerman, J.H. Veerkamp, Cell. Mol. Life. Sci. 59 (2002) 1096–1116.
[7] Z. Zou, F. Tong, N.J. Faergeman, C. Borsting, P.N. Black, C.C. DiRusso, J. Biol. Chem. 278 (2003) 16414–16422.
[8] Y. Wei, D. Wang, F. Topczewski, M.J. Pagliassotti, Am. J. Physiol. Endocrinol. Metab. 21 (2006) 21.
[9] N.H. Haunerland, F. Spener, Prog. Lipid. Res. 43 (2004) 328–349.
[10] E.C. Dell'Angelica, C.A. Stella, M.R. Ermácora, J.A. Santomé, E.H. Ramos, Folia Microbiol. (Praha) 38 (1993) 486–490.
[11] A. Kurlandzka, J. Rytka, R. Gromadka, M. Murawski, Yeast 11 (1995) 885–890.
[12] I. Smaczynska, M. Skoneczny, A. Kurlandzka, Biochem. J. 301 (1994) 615–620.
[13] T.M. Rose, E.R. Schultz, G.J. Todaro, Proc. Natl. Acad. Sci. USA 89 (1992) 11287–11291.
[14] J. Knudsen, N.J. Faergeman, H. Skøtt, R. Hummel, C. Børsting, T.M. Rose, J.S. Andersen, P. Højrup, P. Roepstorff, K. Kristiansen, Biochem. J. 302 (Pt 2) (1994) 479–485.

[15] C.K. Schjerling, R. Hummel, J.K. Hansen, C. Borsting, J.M. Mikkelsen, K. Kristiansen, J. Knudsen, J. Biol. Chem. 271 (1996) 22514–22521.
[16] E.C. Dell'Angelica, M.R. Ermácora, J.A. Santomé, Biochem. Mol. Biol. Int. 39 (1996) 439–445.
[17] L.J. Szabo, G.M. Small, P.B. Lazarow, Gene 75 (1989) 119–126.
[18] H. Tan, K. Okazaki, I. Kubota, T. Kamiryo, H. Utiyama, Eur. J. Biochem. 190 (1990) 107–112.
[19] T. Niki, M. Bun-Ya, Y. Hiraga, Y. Muro, T. Kamiryo, Yeast 10 (1994) 1467–1476.
[20] A.M. Haapalainen, D.M. van Aalten, G. Merilainen, J.E. Jalonen, P. Pirila, R.K. Wierenga, J.K. Hiltunen, T. Glumoff, J. Mol. Biol. 313 (2001) 1127–1138.
[21] F. Leenders, B. Husen, H.H. Thole, J. Adamski, Mol. Cell. Endocrinol. 104 (1994) 127–131.
[22] N.J. Stolowich, A.D. Petrescu, H. Huang, G.G. Martin, A.I. Scott, F. Schroeder, Cell. Mol. Life Sci. 59 (2002) 193–212.
[23] A.M. Gallegos, B.P. Atshaves, S.M. Storey, O. Starodub, A.D. Petrescu, H. Huang, A.L. McIntosh, G.G. Martin, H. Chao, A.B. Kier, F. Schroeder, Prog. Lipid Res. 40 (2001) 498–563.
[24] H. Tan, M. Bun_Ya, A. Hirata, T. Kamiryo, Yeast 10 (1994) 1065–1074.
[25] B. Dujon, D. Sherman, G. Fischer, P. Durrens, S. Casaregola, I. Lafontaine, J. de Montigny, C. Marck, C. Neuveglise, E. Talla, N. Goffard, L. Frangeul, M. Aigle, V. Anthouard, A. Babour, V. Barbe, S. Barnay, S. Blanchin, J.-M. Beckerich, E. Beyne, C. Bleykasten, A. Boisrame, J. Boyer, L. Cattolico, F. Confanioleri, A. de Daruvar, L. Despons, E. Fabre, C. Fairhead, H. Ferry-Dumazet, A. Groppi, F. Hantraye, C. Hennequin, N. Jauniaux, P. Joyet, R. Kachouri, A. Kerrest, R. Koszul, M. Lemaire, I. Lesur, L. Ma, H. Muller, J.-M. Nicaud, M. Nikolski, S. Oztas, O. Ozier-Kalogeropoulos, S. Pellenz, S. Potier, G.-F. Richard, M.-L. Straub, A. Suleau, D. Swennen, F. Tekaia, M. Wesolowski-Louvel, E. Westhof, B. Wirth, M. Zeniou-Meyer, I. Zivanovic, M. Bolotin-Fukuhara, A. Thierry, C. Bouchier, B. Caudron, C. Scarpelli, C. Gaillardin, J. Weissenbach, P. Wincker, J.-L. Souciet, Nature 430 (2004) 35–44.
[26] M.C. Frate, E.J. Lietz, J. Santos, J.P. Rossi, A.L. Fink, M.R. Ermácora, Eur. J. Biochem. 267 (2000) 3836–3847.
[27] J.D. Thompson, T.J. Gibson, F. Plewniak, F. Jeanmougin, D.G. Higgins, Nucleic Acids Res. 25 (1997) 4876–4882.
[28] E.M. Clerico, S.G. Peisajovich, M. Ceolin, P.D. Ghiringhelli, M.R. Ermácora, Biochim. Biophys. Acta 1476 (2000) 203–218.
[29] G. Deleage, C. Geourjon, Comput. Appl. Biosci. 9 (1993) 197–199.
[30] A. Fersht, Structure and Mechanism in Protein Science : A Guide to Enzyme Catalysis and Protein Folding, New York, 1999.
[31] B.M. Cavagnari, D. Milikowski, J.F. Haller, M.C. Zanek, J.A. Santomé, M.R. Ermácora, Int. J. Biol. Macromol. 31 (2002) 19–27.
[32] L.A. Sklar, B.S. Hudson, R.D. Simoni, Biochemistry 16 (1977) 5100–5108.
[33] N.J. Faergeman, B.W. Sigurskjold, B.B. Kragelund, K.V. Andersen, J. Knudsen, Biochemistry 35 (1996) 14118–14126.
[34] D.M. Miller, J.S. Olson, J.W. Pflugrath, F.A. Quiocho, J. Biol. Chem. 258 (1983) 13665–13672.
[35] T. Choinowski, H. Hauser, K. Piontek, Biochemistry 39 (2000) 1897–1902.
[36] D.H. Dyer, S. Lovell, J.B. Thoden, H.M. Holden, I. Rayment, Q. Lan, J. Biol. Chem. 278 (2003) 39085–39091.
[37] T. Szyperski, S. Scheek, J. Johansson, G. Assmann, U. Seedorf, K. Wuthrich, FEBS Lett. 335 (1993) 18–26.
[38] F.L. Garcia, T. Szyperski, J.H. Dyer, T. Choinowski, U. Seedorf, H. Hauser, K. Wuthrich, J. Mol. Biol. 295 (2000) 595–603.
[39] L. Kiemer, J.D. Bendtsen, N. Blom, Bioinformatics 21 (2005) 1269–1270.
[40] G. Neuberger, S. Maurer-Stroh, B. Eisenhaber, A. Hartig, F. Eisenhaber, J. Mol. Biol. 328 (2003) 567–579.
[41] V.N. Uversky, Biochemistry 32 (1993) 13288–13298.
[42] Y. Nozaki, Arch. Biochem. Biophys. 277 (1990) 324–333.
[43] H. Huang, A.M. Gallegos, M. Zhou, J.M. Ball, F. Schroeder, Biochemistry 41 (2002) 12149–12162.
[44] C.W. van Roermund, M. de Jong, L. ljlst, J. van Marle, T.B. Dansen, R.J. Wanders, H.R. Waterham, J. Cell. Sci. 117 (2004) 4231–4237.
[45] J.K. Myers, C.N. Pace, J.M. Scholtz, Protein Sci. 4 (1995) 2138–2148.
[46] A. Frolov, T.H. Cho, J.T. Billheimer, F. Schroeder, J. Biol. Chem. 271 (1996) 31878–31884.
[47] N.J. Stolowich, A. Frolov, B. Atshaves, E.J. Murphy, C.A. Jolly, J.T. Billheimer, A.I. Scott, F. Schroeder, Biochemistry 36 (1997) 1719–1729.
[48] F. Schroeder, A. Frolov, O. Starodub, B.B. Atshaves, W. Russell, A. Petrescu, H. Huang, A.M. Gallegos, A. McIntosh, D. Tahotna, D.H. Russell, J.T. Billheimer, C.L. Baum, A.B. Kier, J. Biol. Chem. 275 (2000) 25547–25555.
[49] F. Schroeder, S.C. Myers-Payne, J.T. Billheimer, W.G. Wood, Biochemistry 34 (1995) 11919–11927.
[50] G. Nemecz, T. Hubbell, J.R. Jefferson, J.B. Lowe, F. Schroeder, Arch. Biochem. Biophys. 286 (1991) 300–309.
[51] M.J. McArthur, B.P. Atshaves, A. Frolov, W.D. Foxworth, A.B. Kier, F. Schroeder, J. Lipid. Res. 40 (1999) 1371–1383.
[52] J.K. Hiltunen, A.M. Mursula, H. Rottensteiner, R.K. Wierenga, A.J. Kastaniotis, A. Gurvitz, FEMS Microbiol. Rev. 27 (2003) 35–64.
[53] P. Fickers, P.H. Benetti, Y. Wache, A. Marty, S. Mauersberger, M.S. Smit, J.M. Nicaud, FEMS Yeast Res. 5 (2005) 527–543.
[54] F.S. Wouters, M. Markman, P. de Graaf, H. Hauser, H.F. Tabak, K.W. Wirtz, A.F. Moorman, Biochim. Biophys. Acta 1259 (1995) 192–196.